Synergy-based Control of Underactuated Anthropomorphic Hands

Fanny Ficuciello, *Senior Member, IEEE*

***Abstract*—In this paper, a grasping control strategy for an anthropomorphic robotic hand in a synergy-based framework is designed. The goal is to achieve a human-like behaviour and robustness with respect to detailed information on objects shape and size. By adapting to underactuated kinematics a well-aimed method for human grasps mapping, the synergies subspace is computed. The designed control strategy allows the hand to adapt to object contours by means of coordinated fingers motion in the synergies subspace, and it is composed of a feedforward and two corrective terms to generate fingertip reference positions. The feedforward term is obtained by choosing, among the configurations contained in the set of grasps used for synergies computation, the one that is closest to the target grasp. This term ensures a suitable pre-shaping of the hand in the synergies subspace on the basis of object and grasp features. On the other hand, in order to adapt the grasp to the object, a weighted sum of two corrective terms is computed using the state of the motors as the feedback of the control law. The first term is designed to generate the closure of the hand towards the object. The second term is designed to optimize a grasp quality index based on force closure property. Moreover, exploiting the motor current feedback, soft synergies are implemented realizing compliance at the contact. The experiments conducted on the underactuated SCHUNK 5-Finger Hand demonstrate the effectiveness of the method.**

***Index Terms*—Bio-inspired control, Anthropomorphic Hands, Dimensionality reduction and underactuation.**

I. Introduction

THE use of anthropomorphic hands has become a key breakthrough in advanced robotics involving both humanoid robots and prosthetic applications. An efficient and forefront design of advanced robotic hands requires solving a compromise among size and weight, functional dexterity and control complexity. A solution to the problem can be found in designing underactuated devices. Basically, this comes down to choosing the optimal number of motors as well as the motion couplings between fingers and joints [1], [2]. A theoretical analysis of underactuated hands has been pointed out in [3] and involves studies on force distribution depending on the mechanical transmissions, design parameters and contact properties. However, underactuated hands require the investigation of planning and control methods that disregard accurate definition of the desired contact points on the object and guarantee robustness with respect to variability of shape and size. Indeed, the inverse kinematics problem hardly has closed form solutions since it is not possible to assign arbitrarily tip positions of all the fingers. Synergies are intended as the correlation between the fingers as well as joint couplings. For this purpose, the synergies paradigm can be exploited as a simplifying tool for planning and control of both fully-actuated and underactuated hands [4]. The synergies concept has also been used to design mechanical couplings for underactuated hands [5]. On the other hand, the compliance at the contact is a fundamental issue to be addressed both from control and design point of view aiming at stable grasping and manipulation abilities [6], [7]. In particular, the concept of soft synergies, providing for compliance during the interaction with the object and the environment, has been introduced in [8] and exploited for robotic hands control [9] and design [10]. Furthermore, the use of synergistic motions is a very promising approach to control not only anthropomorphic hands but more generally high degree-of-freedoms (DoF) devices. Among others, dimensionality reduction of the state space of a mechanical system increases and improves the use of machine learning techniques [11], [12] which allows reaching great results providing robots with skills comparable to human abilities. The use of supervised learning, such as artificial neural networks, or reinforcement learning techniques, serves for the parameterization of synergies depending on task requirements. This allows reproducing biological learning and control that makes human beings so skilled in performing complex manipulation tasks by using a combination of prediction and observation from execution [13]. Another important issue is the use of quality indexes to improve grasping and manipulation performance. Quality measures are used for grasp planning but also for local optimization techniques in case of external disturbance and modeling errors. Most of the quality indexes proposed in the literature determine the proper location of contact points on the object to enhance disturbance resistance property of the grasp [14], as well as proper hand configurations to enhance dexterity property of the grasp [15]. Combinations of quality measures have been also proposed based either on the location of contact points on the object or on the hand configuration [16]. For fully-actuated hands different quality indexes are available in the literature and have been developed mainly for fingertip precision grasps. The extension of these measures for power grasps requires further work and is yet to be done [17]. Very few works have been devoted to the study of grasp properties for underactuated hands. Form closure properties and dexterous manipulation properties have been discussed respectively in [18] and [5]. A study on force closure grasp definition, performed in [19], has been used recently in [20] to implement in MATLAB a force-closure cost function for

The author is an Assistant Professor at PRISMA Lab, University of Naples Federico II (DIETI), via Claudio 21, 80125, Naples, Italy, email: {fanny.ficuciello}@unina.it. The research leading to these results has been partially supported by the RoDyMan project (FP7/2007-2013) under ERC AdG-320992, and partially by MUSHA National Italian project.

Manuscript received January 12, 2018; revised March 12, 2018, accepted May 12, 2018.

underactuated hands. The cost function can be used also in the presence of motor synergies, and, when it is minimized, it allows achieving the best grasp feasible with a given set of synergies. In this paper, a synergy-based control strategy for underactuated anthropomorphic hands is designed and experimentally tested on the SCHUNK five-fingered hand. The synergies subspace for grasping tasks is computed by adapting to underactuated kinematics the method in [21]. Afterwards, a control strategy for both precision and power grasps allowing a local adaptation of the fingertip positions to the object has been developed. Exploiting motor current measurements, a compliance at the contact is ensured while, using motor position measurements, the fingertip reference positions are locally adjusted according to two corrective terms. The first term is designed as a simple strategy to close the hand toward the object. This addresses the lack of detailed information on object shape and size and the difficulty in defining accurately the desired contact points due to the underactuation. The second term is designed to minimize the force closure cost function, defined in [19], with the aim of achieving the best possible grasp locally around the current configuration determined by the pre-shaping term and the first corrective term. The whole control strategy relies on the activation of the first three synergies only and it determines the hand motion and the stable grasping in a reduced dimensional configuration space. The novelty of this approach is that the planning of the grasp relies only on an initial configuration that is learned by imitation from the human. The control strategy designed in this paper is composed of two actions modifying the reference. The two corrections are not related to the object shape and dimension. These actions just rely on proprioceptive sensors of the hand, while the information on object shape and dimension are contemplated only in the initial planned term. The success of the grasp is therefore due to the goodness of the synergies subspace and to the control strategy that optimize a quality index.

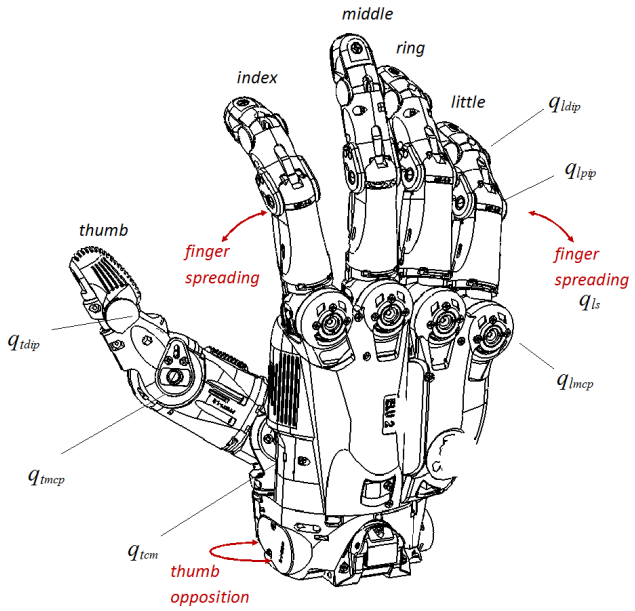

Fig. 1. The finger movement of the Schunk 5 Fingered Hand are illustrated.

II. THE SCHUNK S5FH

The SCHUNK 5-Finger Hand (S5FH) is an anthropomorphic underactuated hand with size, kinematic structure and cosmetic appearance very similar to the human hand. In order to allocate the whole control unit, electronics and mechanical transmissions within the hand and the wrist, underactuation is a suitable solution for optimized mechanical design. The S5FH has 20 joints and 9 DOFs. The whole technical data, hardware and software specifications can be found in [22] and [23].

A. Mechanical Synergies

The number of motors is significantly lower than the number of joints, thus joint motion couplings are regulated by means of mechanical synergies defined via mechanical transmissions. Let $\boldsymbol{q}$ be the vector of the 20 joint angles describing the robotic hand configuration. The number of joints is not the same for each finger as well as the number of DOFs. The thumb has 4 joints (Fig. 1), namely opposition joint q_{t_o}, carpometacarpal flexion joint $q_{t_{cm}}$, metacarpophalangeal flexion joint $q_{t_{mcp}}$, distal interphalangeal flexion joint $q_{t_{dip}}$. The index has 4 joints, namely spread joint q_{i_s}, metacarpophalangeal flexion joint $q_{i_{mcp}}$, proximal interfalangeal flexion joint $q_{i_{pip}}$, distal interphalangeal flexion joint $q_{i_{dip}}$. The middle finger has 3 joints, namely metacarpophalangeal flexion joint $q_{m_{mcp}}$, proximal interfalangeal flexion joint $q_{m_{pip}}$, distal interphalangeal flexion joint $q_{m_{dip}}$. The ring finger has 4 joints, namely spread joint q_{r_s}, metacarpophalangeal flexion joint $q_{r_{mcp}}$, proximal interfalangeal flexion joint $q_{r_{pip}}$, distal interphalangeal flexion joint $q_{r_{dip}}$. The little finger has 4 joints, namely spread joint q_{l_s}, metacarpophalangeal flexion joint $q_{l_{mcp}}$, proximal interfalangeal flexion joint $q_{l_{pip}}$, distal interphalangeal flexion joint $q_{l_{dip}}$. Further, there is one joint allocated into the palm, coupled with the thumb opposition joint, q_{p_o}, that moves only the ring and the little finger with respect to the palm frame. For clearness, the figure lists only the angles of the thumb and the little finger, since for the other fingers they are basically the same. The electric motors control nine coupled motions involving different joints and fingers, namely thumb opposition coupled with the palm joint motion (involving ring and little fingers, 2 DOFs), thumb flexion (3 DOFs), index metacarpophalangeal flexion (1 DOFs), middle metacarpophalangeal flexion (1 DOFs), index proximal/distal flexion (2 DOFs), middle proximal/distal flexion (2 DOFs), fingers spread (index, ring and little, 3 DOFs), ring flexion (3 DOFs) and little finger flexion (3 DOFs). The joint motions are coupled according to the mechanical synergies matrix, defined in (1). In this equation, $\boldsymbol{q} \in \mathbb{R}^{n_q}$, with $n_q = 20$, is the vector of joint variables, $\boldsymbol{m} \in \mathcal{M} \subseteq \mathbb{R}^{n_m}$, with $n_m = 9$, is the vector of motor variables and $\boldsymbol{q}_0$ is a mechanical offset characterizing joint angles when the motor positions are set to zero.

$$\underbrace{\begin{bmatrix} q_{t_o} \\ q_{t_{cm}} \\ q_{t_{mcp}} \\ q_{t_{dip}} \\ q_{i_s} \\ q_{i_{mcp}} \\ q_{i_{pip}} \\ q_{i_{dip}} \\ q_{m_{mcp}} \\ q_{m_{pip}} \\ q_{m_{dip}} \\ q_{p_o} \\ q_{r_s} \\ q_{r_{mcp}} \\ q_{r_{pip}} \\ q_{r_{dip}} \\ q_{l_s} \\ q_{l_{mcp}} \\ q_{l_{pip}} \\ q_{l_{dip}} \end{bmatrix}}_{\boldsymbol{q}} = \underbrace{\begin{pmatrix} 0.5 & 0 & 0 & 0 & 0 & 0 & 0 & 0 & 0 \\ 0 & 0.29 & 0 & 0 & 0 & 0 & 0 & 0 & 0 \\ 0 & 0.29 & 0 & 0 & 0 & 0 & 0 & 0 & 0 \\ 0 & 0.42 & 0 & 0 & 0 & 0 & 0 & 0 & 0 \\ 0 & 0 & 0 & 0 & 0 & 0 & 0 & 0 & 0.25 \\ 0 & 0 & 1 & 0 & 0 & 0 & 0 & 0 & 0 \\ 0 & 0 & 0 & 0.49 & 0 & 0 & 0 & 0 & 0 \\ 0 & 0 & 0 & 0.51 & 0 & 0 & 0 & 0 & 0 \\ 0 & 0 & 0 & 0 & 1 & 0 & 0 & 0 & 0 \\ 0 & 0 & 0 & 0 & 0 & 0.49 & 0 & 0 & 0 \\ 0 & 0 & 0 & 0 & 0 & 0.51 & 0 & 0 & 0 \\ 0.5 & 0 & 0 & 0 & 0 & 0 & 0 & 0 & 0 \\ 0 & 0 & 0 & 0 & 0 & 0 & 0 & 0 & 0.25 \\ 0 & 0 & 0 & 0 & 0 & 0 & 0.26 & 0 & 0 \\ 0 & 0 & 0 & 0 & 0 & 0 & 0.36 & 0 & 0 \\ 0 & 0 & 0 & 0 & 0 & 0 & 0.38 & 0 & 0 \\ 0 & 0 & 0 & 0 & 0 & 0 & 0 & 0 & 0.5 \\ 0 & 0 & 0 & 0 & 0 & 0 & 0 & 0.26 & 0 \\ 0 & 0 & 0 & 0 & 0 & 0 & 0 & 0.36 & 0 \\ 0 & 0 & 0 & 0 & 0 & 0 & 0 & 0.38 & 0 \end{pmatrix}}_{\boldsymbol{S}_m} \underbrace{\begin{bmatrix} m_0 \\ m_1 \\ m_2 \\ m_3 \\ m_4 \\ m_5 \\ m_6 \\ m_7 \\ m_8 \end{bmatrix}}_{\boldsymbol{m}} + \boldsymbol{q}_0 \,. \tag{1}$$

TABLE I
S5FH DENAVIT-HARTENBERG TABLE.

Link (Thumb)	a [mm]	α	d [mm]	θ [deg]
1	0	90	0	0
2	48.50	0	0	0
3	30	0	0	0
4	20	0	0	0
Link (Index)	a [mm]	α	d [mm]	θ [deg]
1	0	90	0	0
2	48.04	0	0	0
3	26	0	0	0
4	15	0	0	0
Link (Middle)	a [mm]	α	d [mm]	θ [deg]
1	50.04	0	0	0
2	32	0	0	0
3	15	0	0	0
Link (Ring)	a [mm]	α	d [mm]	θ [deg]
1	0	90	$-103 + 44.394$	0
2	0	-90	6	-90
3	50.04	0	0	0
4	32	0	0	0
5	15	0	0	0
Link (Little)	a [mm]	α	d [mm]	θ [deg]
1	-21.5	90	$-103 + 44.394 + 9.5$	0
2	0	-90	0	-90
3	44.54	0	0	0
4	22	0	0	0
5	15	0	0	0

B. Kinematics of the SCHUNK S5FH

From the original CAD data of the S5FH the Denavit-Hartenberg parameters of the hand are computed and reported in Table I. Further, the homogeneous transformation matrices between the palm base frame and the fingers base frames, namely $\boldsymbol{T}_t$, $\boldsymbol{T}_i$, $\boldsymbol{T}_m$, $\boldsymbol{T}_r$ and $\boldsymbol{T}_l$ are reported as well.

$$\boldsymbol{T}_t = \begin{pmatrix} 1 & 0 & 0 & 16.90 \\ 0 & \sin(15) & \cos(15) & 45.96\cos(15) \\ 0 & -\cos(15) & \sin(15) & 20.26+45.96\sin(15) \\ 0 & 0 & 0 & 1 \end{pmatrix} ; \; \boldsymbol{T}_i = \begin{pmatrix} 0 & -1 & 0 & 25 \\ 1 & 0 & 0 & 110 \\ 0 & 0 & 1 & 6 \\ 0 & 0 & 0 & 1 \end{pmatrix}$$

$$\boldsymbol{T}_m = \begin{pmatrix} 0 & 0 & 1 & 0 \\ 1 & 0 & 0 & 110 \\ 0 & 1 & 0 & -6 \\ 0 & 0 & 0 & 1 \end{pmatrix} ; \; \boldsymbol{T}_r = \boldsymbol{T}_l = \begin{pmatrix} 1 & 0 & 0 & -18.40 \\ 0 & 0 & -1 & 44.394 \\ 0 & 1 & 0 & 0 \\ 0 & 0 & 0 & 1 \end{pmatrix}$$

Apart from synergies computation, the direct kinematics and the differential kinematics, computed using the Denavit-Hartenberg formulation, are also necessary for the hand control.

C. Differential Kinematics

The differential kinematics between the mechanical synergies subspace and the Cartesian space, is represented by the following equation $\dot{\boldsymbol{x}} = \boldsymbol{J}_{h_m} \dot{\boldsymbol{m}}$, where $\boldsymbol{J}_{h_m} \in \mathbb{R}^{n_x \times n_m}$ is the mechanical synergies Jacobian and is computed as $\boldsymbol{J}_{h_m} = \boldsymbol{J}_h \boldsymbol{S}_m$, such that,

$$\dot{\boldsymbol{x}} = \boldsymbol{J}_h \boldsymbol{S}_m \dot{\boldsymbol{m}} = \boldsymbol{J}_h \dot{\boldsymbol{q}}; \tag{2}$$

$\boldsymbol{x} \in \mathbb{R}^{n_x}$, with $n_x = 15$, is the position vector of the five fingertips, $\boldsymbol{J}_h \in \mathbb{R}^{n_x \times n_q}$ is the S5FH hand Jacobian. $\boldsymbol{S}_m \in \mathbb{R}^{n_q \times n_m}$ is the matrix of the mechanical synergies and maps motor velocities into joint velocities, $S_m \dot{\boldsymbol{m}} = \dot{\boldsymbol{q}}$.

III. SYNERGIES SUBSPACE COMPUTATION

In addition to the mechanical synergies of the hand, motion coordination patterns or motor synergies can be computed to further reduce the number of parameters needed to plan and control the grasping activities. Synergies subspace for hand control has been computed using human grasp data and a mapping algorithm available from a previous work developed in [24]. Human grasps data are based on fingertips measurements that are used as desired references in a closed-loop inverse kinematics (CLIK) scheme that is in charge of reconstructing the hand configuration. Since significant differences exists in both the size and the kinematics of the human hands, the method has been applied to 5 different subjects for mapping generalization of each grasps in the chosen database. For further investigation the reader is directed to the works [21], [24]. The extension of the method to underactuated hands implies solving an inverse kinematics problem where the Jacobian is a high-rectangular matrix, which is typical when the number of equations is greater than the number of the unknown variables. In this case, the solution to the inverse problem does not exist if the position vector of the fingetips $\boldsymbol{x} \notin \Re(\boldsymbol{J}_{h_m})$, but only an approximate solution can be found. Indeed, despite similar kinematics, the actuation dissimilarity leads to workspaces of the human and robotic hand with different shape and size.

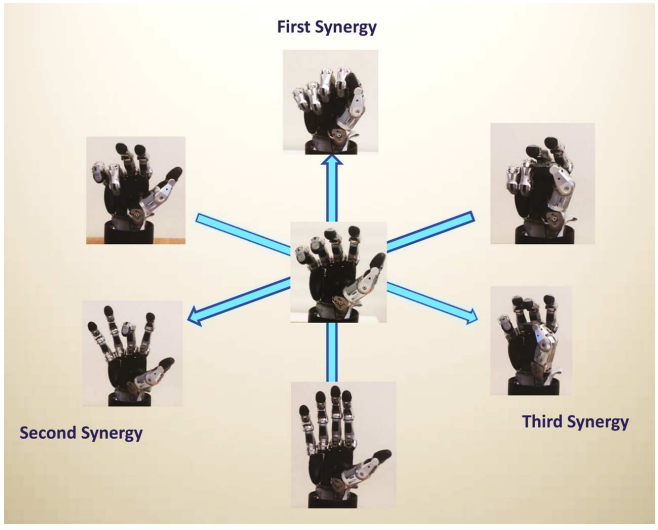

Fig. 2. The first three eigengrasps.

Because of the underactuation, whatever the mapping method of human hand motion to the robotic hand, a faithful mapping will never be achieved and part of the information will be unavoidably lost.

Besides the method of mapping the grasps from the human

hand, there is another possibility to compute the synergies subspace, i.e. the grasping postures can be produced directly on the robotic hand by driving each motor using a sliding guide.

In this case, the reference set should be adapted to the motion ability of the robotic hand. Furthermore, the computed subspace will strongly depend on the operator abilities and personal preferences in defining a natural grasp.

Thus, in the first case, using measurements on five human subjects, it is possible to compute a synergies subspace allowing generalization of grasp synthesis, in the second case the results will be strongly operator dependent and limited to few grasps. The maps between the synergies subspace and the motor space, and between the synergies subspace and the joint space are given respectively by $\boldsymbol{m} = \boldsymbol{S}_s\boldsymbol{\sigma} + \bar{\mathbf{m}}$, and $\boldsymbol{q} = \boldsymbol{S}_m(\boldsymbol{S}_s\boldsymbol{\sigma} + \bar{\mathbf{m}}) + \boldsymbol{q_0}$.

The matrix $\boldsymbol{S}_s \in \mathbb{R}^{n_m \times n_s}$ represents the base of the synergies subspace, whose dimensions depend on the number of eigengrasps considered to approximate the grasp. Thus, the number n_s can vary from 1 to 9. In this work, the synergies subspace is three-dimensional and, thus, it is obtained by choosing $n_s = 3$. Thus, the columns are the first three eigenvectors (or eigengrasps) with higher variance computed using principal component analysis (PCA) on the grasps dataset mapped from the human hand to the robotic hand. Finally, $\bar{\mathbf{m}} \in \mathcal{M} \subseteq \mathbb{R}^{\mathbf{n_m}}$ is the zero-offset of the motor synergies subspace.

The results on synergies computation are reported in Fig. 2, where the synergies subspace is synthetically represented. On the three principal axes of the eigengrasps, the configurations that the hand assumes accordingly to the patterns of the first, second and third synergies, are reported. The synergy coefficients vary from a minimum to a maximum value in agreement with the positive direction of the axis arrows. The axes, representing the eigenvectors of the synergies subspace, are oriented taking into account the sign of the coefficients. When the coefficients are all zero the hand is in the home position which represents the origin of the synergies subspace and which is represented at the center of the figure.

IV. Control in the Synergies Subspace

Neuroscience studies reveal that human beings realize grasping actions by means of a first step of pre-shaping, exploiting synergies, learning strategies and vision, and a second phase of adaptation to the object that requires mainly contact forces sensory information [25]. The best practice to provide a robotic manipulation system of autonomous capabilities is to imitate human sensory-motor behaviour. The idea of the control strategy is schematically represented in Fig. 3. An artificial brain (represented by the PC in the Figure) should provide high level model-based algorithm for object recognition and even for scene interpretation, allowing evaluation of grasping affordance. The identified object/grasp, among the example available in a data-base, can be used as reference for hand pre-shaping control (preshaping hand configuration represented on the left in the Figure). Afterwords, the local adaptation and optimization of the grasp can be realized in a synergy-based framework exploiting mainly force and position feedback (final hand configuration represented on the right in the Figure).

In this work, a control strategy for autonomous grasping has been developed as a dowel of the whole framework described above. Starting from a suitable pre-shaping configuration and moving in a subspace of reduced dimensions, the hand can autonomously adapt to any kind of object using the proprioceptive sensors supplied with it.

Fig. 3. Scheme of the autonomous grasping strategy.

The grasping control is performed in the Cartesian space with a scheme that uses the transpose of the synergies Jacobian, defining the differential kinematics between the motor synergies subspace and the Cartesian space $\dot{\boldsymbol{x}} = \boldsymbol{J}_{h_{m_s}}\dot{\boldsymbol{\sigma}}$, where $\boldsymbol{J}_{h_{m_s}} \in \mathbb{R}^{n_x \times n_s}$ is the synergies Jacobian and is computed as $\boldsymbol{J}_{h_{m_s}} = \boldsymbol{J}_h\boldsymbol{S}_m\boldsymbol{S}_s$, and $\dot{\boldsymbol{m}} = \boldsymbol{S}_s\dot{\boldsymbol{\sigma}}$ is the differential map between the motor synergies and the mechanical synergies obtained by deriving $\boldsymbol{m} = \boldsymbol{S}_s\boldsymbol{\sigma} + \bar{\mathbf{m}}$. The linear maps relating the velocities in motor synergy coordinates and mechanical synergy coordinates, and at joint and Cartesian level are depicted in Fig. 4. With the aid of set theory, the previous equations are synthesized in a comprehensive representation.

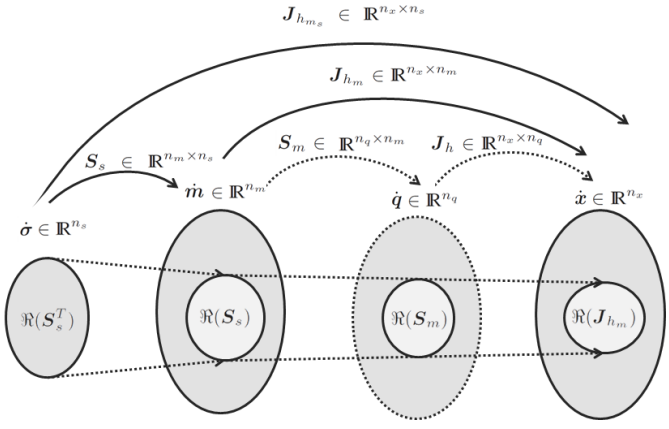

Fig. 4. Linear maps relating the velocities in motor synergy coordinates and mechanical synergy coordinates, and at joint and Cartesian level.

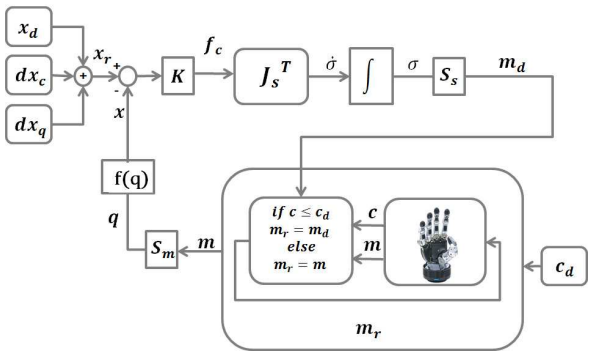

Fig. 5. Block scheme of the control strategy.

The scheme of the control strategy applied to the SCHUNK 5-Finger Hand is presented in Fig. 5.

In details, the feedforward term of the control strategy, $\boldsymbol{x}_d$, represents the configuration selected within the data-set used for synergies computation on the basis of the similarities related to the object shape and size, and to the grasp type, namely power, precision or lateral grasp [26]. This configuration, approximated with the first three synergies, ensures the correct pre-shaping of the hand in the three-dimensional synergies subspace. The approximation in the synergies subspace is obtained by reproducing the configuration using $\boldsymbol{q} = \boldsymbol{S}_m(\boldsymbol{S}_s\boldsymbol{\sigma}+\bar{\mathbf{m}})+\boldsymbol{q_0}$, where the snergies matrix, $\boldsymbol{S}_s \in \mathbb{R}^{n_m \times n_s}$, is chosen with three columns, i.e. with $n_s = 3$. For local adaptation, two corrective terms are implemented relying on motor current and position measurements. The object recognition and the association with a target in the reference set of grasps can be obtained by using an expert vision system [27]. In the following, the two corrective terms are described, as well as the force synergies generation. Finally, stability remarks are presented.

A. Correction to close the hand adapting to the object

For each grasping task, the initial configuration, from which the hand starts to move, is given by $\boldsymbol{q}_0$, i.e. the zero offset of the hand corresponding to motor positions set to zero ($\boldsymbol{m} = \mathbf{0}$). In the Cartesian space, using direct kinematics, the initial fingertip positions is given by the vector $\boldsymbol{x}_0 = \boldsymbol{f}(\boldsymbol{q}_0)$. During the fingers' motion from the initial configuration to the desired one $\boldsymbol{x}_d$, at each sample time the reference position is corrected by adding a term. This correction term is a constant gain multiplied for the unit vector oriented from the actual fingertip positions to the mean position of the fingertips employed in the grasp. In the formula this point is represented by $\mathbf{obj_c}$ as to indicate the centroid of a virtual object builded on the fingertips employed in the grasp. Let $\boldsymbol{x}_d = [\boldsymbol{x}^{t^T}, \boldsymbol{x}^{i^T}, \boldsymbol{x}^{m^T}, \boldsymbol{x}^{r^T}, \boldsymbol{x}^{l^T}]^T \in \mathbb{R}^{n_x}$ be the vector of the fingertip positions in the Cartesian space and let indicate $\boldsymbol{x}^f$ the generic fingertip, with $f \in \{t, i, m, r, l\}$. The corrective term for each fingertip is given by

$$d\boldsymbol{x}_c^f = \alpha_c \frac{\mathbf{obj_c} - \boldsymbol{x}^{\mathbf{f}}}{\|\mathbf{obj_c} - \boldsymbol{x}^{\mathbf{f}}\|} \tag{3}$$

where α_c is a positive gain chosen experimentally, while $\mathbf{obj_c}$ is the point representing the mean position of the fingers employed in the grasp.

B. Correction based on the quality of the grasp

A synergy-based quality index, that relies on the force-closure property investigated in [19], is adopted in the role of a cost function, V, to be minimized in order to increase the quality of the grasp. The general solution for the set of contact forces balancing an object grasped by a robotic hand with n_c contact points is: $\boldsymbol{f} = \boldsymbol{G}^{\dagger}\boldsymbol{w} + \boldsymbol{E}\delta\boldsymbol{q}$, where $\boldsymbol{f} \in \mathbb{R}^{3n_c}$ is the vector collecting the contact forces applied at the n_c contact points, $\boldsymbol{w} = (\boldsymbol{f}_o^T, \boldsymbol{\mu}^T)^T \in \mathbb{R}^6$ is the external load, where $\boldsymbol{f}_o \in \mathbb{R}^3$ and $\boldsymbol{\mu} \in \mathbb{R}^3$ are respectively the external force and moment acting on the object, $\boldsymbol{G}^{\dagger}$ is a right-pseudoinverse of the grasp matrix $\boldsymbol{G}$, $\boldsymbol{E}$ is a basis for the subspace of controllable internal forces, and finally $\delta\boldsymbol{q}$ is the joint reference displacements. The matrix $\boldsymbol{E}$ maps the controlled joint displacement into internal forces activated on the object. Underactuation reduce the subspace's dimension of controllable internal forces according to the mechanical and motor synergies and, thus, according to the matrices $\boldsymbol{E}_m = \boldsymbol{E}\boldsymbol{S}_m$ and $\boldsymbol{E}_s = \boldsymbol{E}\boldsymbol{S}_m\boldsymbol{S}_s$.

By rewriting $\boldsymbol{q} = \boldsymbol{S}_m(\boldsymbol{S}_s\boldsymbol{\sigma} + \bar{\mathbf{m}}) + \boldsymbol{q_0}$ in the case of elementary displacement, the following holds: $\delta\boldsymbol{q} = \boldsymbol{S}_m\delta\boldsymbol{m} = \boldsymbol{S}_m\boldsymbol{S}_s\delta\boldsymbol{\sigma}$. The general solution of the grasping problem in terms of a synergistic approach can be obtained as $\boldsymbol{f} = \boldsymbol{G}^{\dagger}\boldsymbol{w} + \boldsymbol{E}_s\delta\boldsymbol{\sigma}$.

Starting from the general grasping problem of $\boldsymbol{f} = \boldsymbol{G}^{\dagger}\boldsymbol{w} + \boldsymbol{E}_s\delta\boldsymbol{\sigma}$, and applying Coulomb's inequality for friction constraints fulfillment, a quality index for force-closure has been defined in [19]. Without going into details, an algorithm for optimal force distribution towards the improvement of force closure property can be based on the minimization of a cost function $V(\delta\boldsymbol{\sigma})$ with respect to $\delta\boldsymbol{\sigma}$.

Let $\Omega_{i,j}^k \subset \mathbb{R}^h$ indicate the set of grasp variables $\boldsymbol{y}$ that satisfy the friction cone constraint with a (small, positive) margin k, where h is the dimension of $\boldsymbol{E}$.
For the $i-th$ contact and the $j-th$ constraint, V is obtained as the summation of the terms: $V(\boldsymbol{w}, \boldsymbol{y}) = \sum_i \sum_j V_{i,j}(\boldsymbol{w}, \boldsymbol{y})$, defined as

$$V_{i,j} = \begin{cases} (2\sigma_{i,j}^2(\boldsymbol{w}, \boldsymbol{y}))^{-1} & \boldsymbol{y} \in \Omega_{i,j}^k, \\ a\sigma_{i,j}^2(\boldsymbol{w}, \boldsymbol{y}) + b\sigma_{i,j}(\boldsymbol{w}, \boldsymbol{y}) + c & \boldsymbol{y} \notin \Omega_{i,j}^k \end{cases}, \tag{4}$$

where a, b and c are constant positive parameters conditioned by properties imposed to V.

This cost function, detailed in [19] and [8], has a formulation, suitable for practical implementation in manipulation planning. To be more specific, the function V has been adopted as a cost function indicating the quality of grasp since the reciprocal of V reflects the distance of the grasp from violating the friction cone constraints and is obtained by formulating and solving the problem as a second order cone programming (SOCP).

Therefore, in this work in order to minimize the cost function and increase the force-closure properties of the target grasp, a second corrective term has been added to the planned

desired reference. The term is designed in order to move the fingertip reference positions toward the opposite direction of the gradient of V. The idea is to generate synergistic motions that minimize this cost function

$$\dot{\boldsymbol{\sigma}} = \alpha_q \frac{\partial V}{\partial \boldsymbol{\sigma}}, \tag{5}$$

where the synergy velocities $\dot{\boldsymbol{\sigma}}$ are computed as (see Fig. 5) $\dot{\boldsymbol{\sigma}} = \boldsymbol{J}_{h_{m_s}}^T \boldsymbol{K}(\boldsymbol{x}_r - \boldsymbol{x})$, where $\boldsymbol{x}_r = \boldsymbol{x}_d + d\boldsymbol{x}_c + d\boldsymbol{x}_q$ is the reference position of the fingertips,

$$d\boldsymbol{\sigma} = \alpha_q \frac{\partial V}{\partial \boldsymbol{\sigma}} dt, \tag{6}$$

and the gradient of V is computed numerically and multiplied for a constant gain $\alpha_q < 0$. The matrix $\boldsymbol{K} \in \mathbb{R}^{n_x \times n_x}$ is the proportional gain multiplying the position error of the controlled system, and can be written as $\boldsymbol{K} = k\boldsymbol{I}_{n_x \times n_x}$ where $\boldsymbol{I}_{n_x \times n_x}$ is the n_x-dimensional identity matrix and $k \in \Re$ is a scalar chosen to comply stability issues. To obtain the fingertip correction the following equation holds

$$d\boldsymbol{x} = \alpha_q \boldsymbol{J}_{h_{m_s}} \frac{\partial V}{\partial \boldsymbol{\sigma}} dt \tag{7}$$

By normalizing the vector $d\boldsymbol{x}$ with respect its norm, the CLIK reference is given by

$$d\boldsymbol{x}_q = \alpha_q \frac{d\boldsymbol{x}}{\|d\boldsymbol{x}\|} \tag{8}$$

where $\alpha_q < 0$ has been chosen experimentally.

C. Force synergies generation using motor current thresholds

The contact forces, to hold the object in a stable grasp, are generated in the control strategy by means of the error between the reference position and the effective position of the fingertips in the Cartesian space.

In the CLIK scheme, the proportional control action $\boldsymbol{K}(\boldsymbol{x}_r - \boldsymbol{x}) = \boldsymbol{f}_c$ has a physical interpretation. Indeed, $\boldsymbol{f}_c \in \mathbb{R}^{n_x}$ can be seen as a vector collecting the elastic reaction forces generated by 3D linear springs positioned between the desired and the actual position of the fingertips, with stiffness $\boldsymbol{K}^f = k\boldsymbol{I}_{3\times 3}$, being $\boldsymbol{I}_{3\times 3}$ the 3-dimensional identity matrix and $f \in \{t, i, m, r, l\}$. The kineto-static duality between generalized forces and velocities holds also between the synergistic forces and synergistic displacements. Since, from $\dot{\boldsymbol{m}} = \boldsymbol{S}_s \dot{\boldsymbol{\sigma}}$ and $\dot{\boldsymbol{x}} = \boldsymbol{J}_{h_m} \dot{\boldsymbol{m}}$ we obtain $\dot{\boldsymbol{x}} = \boldsymbol{J}_{h_m} \boldsymbol{S}_s \dot{\boldsymbol{\sigma}}$, it holds $\boldsymbol{\eta} = \boldsymbol{S}_s{}^T \boldsymbol{\tau}_m = \boldsymbol{S}_s{}^T \boldsymbol{J}_{h_m}{}^T \boldsymbol{f}$, where $\boldsymbol{\eta} \in \mathbb{R}^{n_s}$ is the vector of the force synergies.

In Fig. 6, the kineto-static duality and the relations between the image space and null space of the $\boldsymbol{S}_s$ and $\boldsymbol{J}_{h_m}$ maps are highlighted. In order to limit the contact forces, thresholds $\boldsymbol{c}_d$ on the motor current $\boldsymbol{c}$ are established experimentally. When a motor current exceeds the threshold the control freezes the reference desired position $\boldsymbol{m}_d$ at the previous value. Therefore, the motor holds the current position $\boldsymbol{m}$ and velocity goes to zero. Hence, the error between the reference position and the current position of the fingertips remains constant as well as the contact forces generated by the control action. In this work, compliance at the contact, determined by both the object and soft-pad elasticity, and compliance at the joints are not included in the analysis even if they affect the contact forces model and should be considered in a detailed analysis of force and motion controllability. This omission is due to the fact that the contact forces and the internal forces are not controlled to a reference value because a direct measure of the contact forces is not available. Therefore, the control just provide a contact force limitation according to a preplanned current threshold.

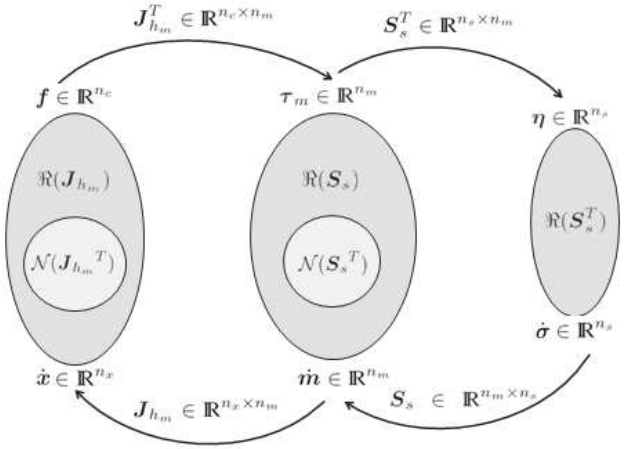

Fig. 6. The kineto-static duality between the generalized forces and velocities

D. Stability remarks

The stability proof of the CLIK algorithms has been widely provided for both the continuous and discrete time using Lyapunov theory and alternative approaches as in [28]. Since the Jacobian is a high-rectangular matrix, the solution to the inverse problem does not exist if the position vector of the fingetips $\boldsymbol{x} \notin \Re(\boldsymbol{J}_{h_m})$. Therefore, the convergence of the error can be ensured to a finite value depending on the approximate solution given by the CLIK algorithm. To ensure stability, the proportional control gain $\boldsymbol{K}$ is chosen with the scalar k limited by the inverse of the sample time T and a scalar δ chosen as $\delta > 0 : \left\|\boldsymbol{J}_{h_{m_s}}(\boldsymbol{m})\right\| \leq \delta \forall m \in \mathcal{M}$, such that $0 < k < \frac{1}{T\delta^2}$. Moreover, the initial value and the dynamics of the position error are limited by normalizing the two correction terms, as in (3) and (8), and by limiting the parameters α_c and α_q.

In Fig. 7, the synergy coefficients are reported for a cylindrical grasp. It is possible to observe that the control modifies the synergy coefficients until stably reaching a steady-state value which depends on the current thresholds, chosen empirically to limit the contact forces based on the fragility and weight of the objects. Considering the objects involved in the experiments, the thresholds have been chosen the same for each grasp.

V. Experimental Results

The Robot Operating System (ROS) is used to control the SCHUNK 5-Finger Hand. A SVH Driver suite has been developed by FZI Forschungszentrum Informatik for the low level interface and enables an easy control of the hand using a customized library written in C++. In this section, the experimental results of the proposed synergy-based control

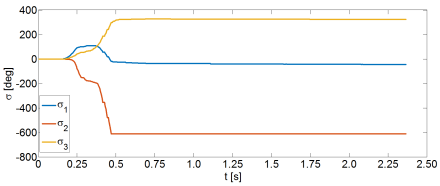

Fig. 7. Time history of synergy coefficients during grasping a cylindrical object.

strategy are presented. With respect to a previous work [26], the underactuation of the robotic hand leads to loss of information when human grasps are mapped on the robotic hand. Therefore, the computed synergies subspace does not allow reproducing precisely the grasps only by projection of the original human hand configuration. By looking at Fig. 8, where hand preshaping configurations for different objects' grasping are represented, it is evident that the method allows a good preshaping for each object shape.

On the other hand, in order to appreciate the grasp stability improvement, given by the use of the quality index, the grasps obtained with the local adaptation based only on the corrective term of eq. (3) are compared with the grasps obtained by optimizing also the quality index. It is evident that for both precision grasps in Fig. 9 and power grasp in Fig. 10 the fingers are more uniformly distributed around the object (images on the right in the figures). Indeed, the area of the polygon formed by the three contact points increases in the case of tripodal grasp, the shape of the grasp polygon improves in the case of a five-fingers grasp and, finally, the minimum distance between the centroid of the object and the line that connects thumb and index contact points in the case of bipodal grasp is reduced. About the lateral grasp in Fig. 11, only the control strategy with quality index optimization leads to a successful grasp.

This demonstrates that the sole centroid criterion as correction for the pre-shaping term is not always sufficient to stably grasp an object. In order to carry out a quantitative evaluation, the quality index of the grasp has been calculated using Syngrasp simulator [20] in both cases and reported in Table II. The stability improvement is proved by the reduced value of the quality index optimized by the control strategy, as evident from the figures.

In Fig. 12 four different object grasps obtained starting from the same hand pre-shaping and using the synergy-based control with force closure optimization are shown.

A wide variety of grasps executed controlling the hand in the synergies subspace using both the corrections terms are reported in Fig. 13. It is possible to appreciate the effectiveness of the proposed control strategy for different kind of objects and grasp types.

Fig. 8. Hand preshaping for a wide variety of grasps.

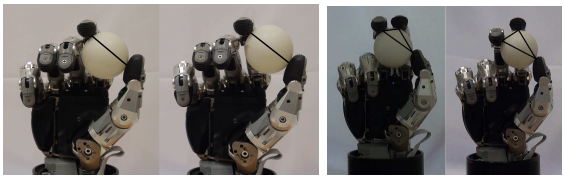

Fig. 9. Bipodal and tripodal grasps executed in the synergies subspace. On the right the force closure cost is optimized.

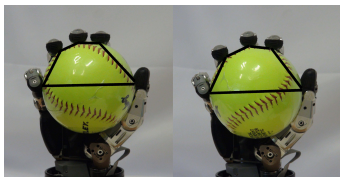

Fig. 10. Five-finger power grasp reproduced in the synergies subspace. On the right the force closure cost is optimized.

TABLE II
QUANTITATIVE COMPARISON BETWEEN THE TWO CONTROL LAWS USING THE FORCE-CLOSURE QUALITY INDEX [19].

	Quality Index Value	
Grasp	Centroid	Centroid + Quality Index Gradient
Bipodal	$1.9 \cdot 10^7$	$8.5 \cdot 10^5$
Tripodal	$2.5 \cdot 10^7$	$3.1 \cdot 10^6$
Sphere five finger	$2.7 \cdot 10^8$	$4.6 \cdot 10^7$
Cylinder five finger	$1.9 \cdot 10^8$	$1.4 \cdot 10^7$
Lateral	- -	$2.7 \cdot 10^6$

To ensure that the execution of the grasp is not affected by the intervention of the operator, and to be able to compare the results in the two different control choices, we use different supports for holding up the objects. The supports are appropriate to the grasp to be executed. Moreover, for different trials the object is always disposed in the same position that has been chosen suitably as to make the grasp possible. In Fig. 14 examples of different solutions for different grasps are reported.

VI. CONCLUSIONS AND FUTURE WORK

In this work, a synergy-based control strategy for autonomous grasping has been implemented. An underactuated hand, the SCHUNK S5FH, has been used for experimental test. A synergies computation algorithm has been adapted for underactuated kinematics and the results demonstrate the goodness of the computed synergies subspace for hand control. A suitable pre-shaping configuration has been selected among the reference set of grasps used for synergies computation and used as feedforward term of the control strategy. Two terms, to adapt on-line the desired reference grasp to the object, have been computed according to a strategy to close the hand toward the object, and a strategy to optimize a quality index. The whole control law runs in the three-dimensional synergies subspace and implement soft contact exploiting motor current measurements. Future works will introduce vision algorithm and learning strategies for object recognition and optimized hand pre-shaping.

Fig. 11. Lateral side grasp executed in the synergies subspace with and without force closure optimization are reported respectively on the left and right side of the figure.

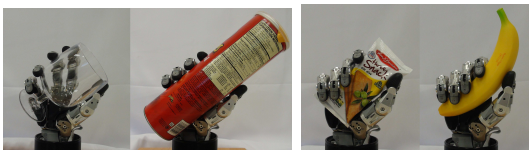

Fig. 12. Cylindrical grasps executed in the synergies subspace starting from the same hand pre-shaping.

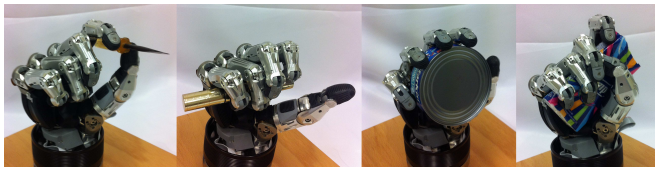

Fig. 13. A wide variety of grasps are executed in the synergies subspace with the proposed control strategy.

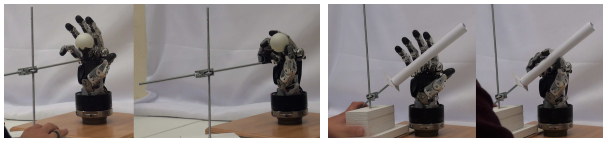

Fig. 14. Some examples of the different solution used as a support for holding up the objects.

REFERENCES

[1] D. M. Aukes, B. Heyneman, J. Ulmen, H. Stuart, M. R. Cutkosky, S. Kim, P. Garcia, and A. Edsinger, "Design and testing of a selectively compliant underactuated hand," *The International Journal of Robotics Research*, vol. 33, no. 5, pp. 721–735, 2014.

[2] R. Deimel and O. Brock, "A novel type of compliant and underactuated robotic hand for dexterous grasping," *The International Journal of Robotics Research*, vol. 35, no. 1-3, pp. 161–185, 2016.

[3] L. Birglen, T. Laliberté, and C. Gosselin, *Underactuated Robotic Hands*, ser. Springer Tracts in Advanced Robotics, O. Khatib, V. Kumar, and G. Pappas, Eds. Springer Berlin / Heidelberg, 2008, vol. 40.

[4] J. Romero, T. Feix, C. H. Ek, H. Kjellstrom, and D. Kragic, "Extracting postural synergies for robotic grasping," *IEEE Transactions on Robotics*, vol. 29, no. 6, pp. 1342–1352, 2013.

[5] L. U. Odhner and A. Dollar, "Dexterous manipulaion with underactuated robotic hands," in *Proc. IEEE Int. Conf. on Robotics and Automation*, Shanghai, China, 2011.

[6] F. Ficuciello, R. Carloni, L. Visser, and S. Stramigioli, "Port-hamiltonian modeling for soft-finger manipulation," in *Proc IEEE/RSJ Int Conf on Intelligent Robots and Systems*, Taipei, Taiwan, 2010, pp. 4281–4286.

[7] H. Deng, G. Zhong, X. Li, and W. Nie, "Slippage and deformation preventive control of bionic prosthetic hands," *IEEE/ASME Trans. Mechatronics*, 2017.

[8] M. Gabiccini and A. Bicchi, "On the role of hand synergies in the optimal choice of grasping forces," in *Proc. of Robotics: Science and Systems*, Zaragoza, 2010.

[9] T. Wimboeck, B. Jan, and G. Hirzinger, "Synergy-level impedance control for a multifingered hand," in *Proc. IEEE Int. Conf. on Intelligent Robots and Systems*, San Francisco, 2011, pp. 973–979.

[10] C. D. Santina, G. Grioli, M. Catalano, A. Brando, and A. Bicchi1, "Dexterity augmentation on a synergistic hand: The Pisa/IIT SoftHand+," in *Proc IEEE-RAS 15th Int Conf on Humanoid Robots*, Seoul, Corea, 2015, pp. 497–503.

[11] F. Ficuciello, D. Zaccara, and B. Siciliano, "Synergy-based policy improvement with path integrals for anthropomorphic hands," in *Proc IEEE Int Conf on Intelligent Robots and Systems*, Daejeon, Korea, 2016, pp. 1940–1945.

[12] ——, *Learning Grasps in a Synergy-based Framework*, ser. Springer Proceedings in Advanced Robotics. Springer, 2017, ch. 2016 Int Symposium on Experimental Robotics.

[13] R. Shadmehr and S. Mussa-Ivaldi, in *Biological Learning and Control: How the Brain Builds Representations, Predicts Events, and Makes Decisions*. MIT Press, 2012.

[14] J. Cornella and R. Suarez, "Fast and flexible determination of force-closure independent regions to grasp polygonal objects," in *Proc. IEEE Int. Conf. on Robotics and Automation*, Barcelona, Spain, 2005, pp. 778–783.

[15] D. Prattichizzo, M. Malvezzi, M. Gabiccini, and A. Bicchi, "On motion and force controllability of precision grasps with hand actuated by soft synergies," *IEEE Transactions on Robotics*, vol. 29, no. 6, pp. 1440–1456, 2010.

[16] B. Leon, J. Sancho-Bru, N. Jarque-Bou, A. Morales, and M. Roa, "Evaluation of human prehension using grasp quality measures," *International Journal of Advanced Robotic Systems*, vol. 9, pp. 1–12, 2012.

[17] M. Roa and R. Suarez, "Grasp quality measures: review and performance," *Autonomous Robots*, vol. 38, no. 1, pp. 65–88, 2015.

[18] S. Krut, V. Begoc, E. Dombre, and F. Pierrot, "Extension of the form closure property to underacuated hands," *IEEE Transactions on Robotics*, vol. 26, pp. 853–866, 2010.

[19] A. Bicchi, "On the closure properties of robotic grasping," *International Journal of Robotics Research*, vol. 14, no. 4, pp. 319–334, 1994.

[20] M. Malvezzi, G. Gioioso, G. Salvietti, and D. Prattichizzo, "Syngrasp: A matlab toolbox for underactuated and compliant hands," *IEEE Robotics and Automation Magazine*, vol. 22, no. 4, pp. 52–68, 2015.

[21] F. Ficuciello, G. Palli, C. Melchiorri, and B. Siciliano, "A model-based strategy for mapping human grasps to robotic hands using synergies," in *Proc IEEE/ASME International Conference on Advanced Intelligent Mechatronics (AIM)*, Wollongong, Australia, 2013, pp. 1737–1742.

[22] "Schunk hand webpage," http://mobile.schunk-microsite.com/en/produkte/produkte/servoelektrische-5-finger-greifhand-svh.html.

[23] "schunk_svh_driver," http://wiki.ros.org/schunk_svh_driver.

[24] G. Palli, C. Melchiorri, G. Vassura, and U. S. et al., "The dexmart hand: Mechatronic design and experimental evaluation of synergy-based control for human-like grasping," *Int Journal of Robotics Research*, vol. 33, pp. 799–824, 2014.

[25] T. Iberall, "Human prehension and dexterous robot hands," *International Journal of Robotics Research*, vol. 16, no. 3, pp. 285–299, 1997.

[26] F. Ficuciello, G. Palli, C. Melchiorri, and B. Siciliano, "Postural synergies of the UB Hand IV for human-like grasping," *Robotics and Autonomous Systems*, vol. 62, pp. 357–362, 2014.

[27] B. Browatzki, V. Tikhanoff, G. Metta, H. Bülthoff, and C. Wallraven, "Active object recognition on a humanoid robot," in *Proc. IEEE Int. Conf. on Robotics and Automation*, Saint Paul, Minnesota, 2012, pp. 2021–2028.

[28] P. Falco and C. Natale, "On the stability of closed-loop inverse kinematics algorithms for redundant robots," *IEEE Transactions on Robotics*, vol. 27, no. 4, pp. 780–784, 2011.

Fanny Ficuciello received the Laurea degree magna cum laude in Mechanical Engineering and the Ph.D. degree in Computer and Automation Engineering both from the University of Naples Federico II. Currently she is an Assistant Professor at the University of Naples Federico II. Her research activity is focused on biomechanical design and bio-aware control strategies for anthropomorphic hands, grasping and manipulation, human–robot interaction, variable impedance control, redundancy resolution and surgical robotics. She has published more than 30 journal, conference papers and book chapters. She is the recipient of a National Grant under which she is the PI of the MUSHA project (http://www.musha.unina.it/). She serves as an associate editor of the Journal of Intelligent Service Robotics.